strong indication of the importance of electron–electron correlation effects[27].

We have shown that one can continuously and reversibly move through the metal-insulator transition by simply changing the hydrogen to yttrium ratio from 1.8 to 2.9 in yttrium thin films, covered by a palladium overlayer. This can be done in a remarkably short time by just changing the pressure of the hydrogen gas surrounding the sample at room temperature. The spectacular changes in optical properties (from a shiny mirror to a yellow transparent window) could potentially lead to technological applications of metal-hydride films because: (1) P. H. L. Notten *et al.* (manuscript in preparation) have found that our samples can easily be charged electrolytically and (2) M. Ouwerkerk *et al.*, (manuscript in preparation found in the hydrides of some RE alloys optical switching times much faster than those of YH_x and LaH_x. We have determined the direct energy gap of YH_3 (1.8 eV); its magnitude disagrees with recent band-structure calculations[25,26] that predict a (semi) metallic ground state, and is far too large for an excitonic insulator[28]. Our results strongly suggest that electron correlation effects are important in YH_x, LaH_x and REH_x.

Because the electrical and optical phenomena are not limited to yttrium and lanthanum, but are also found in rare earths and their alloys, the technique used in this work offers many possibilities of unravelling the intriguing properties of trihydrides and non-stoichiometric higher hydrides, MH_x, in general. □

Received 6 October 1995; accepted 1 February 1996.

1. Mott, N. F. in *Metal-Insulator transitions* 2nd edn (Taylor & Francis, London 1990).
2. Verleur, H. W., Barker, A. S. Jr & Berglund, C. N. *Phys. Rev.* **172,** 788–798 (1968).
3. Libowitz, G. G. *Ber. Bunsenges. phys. Chem.* **77,** 837–845 (1973).
4. Libowitz, G. G. & Maeland, A. J. in *Handbook on the Physics and Chemistry of Rare Earths* (eds Gschneidner, K. A. & Eyring, L.) 299–336 (North Holland, Amsterdam, 1979).
5. Vajda, P. in *Handbook on the Physics and Chemistry of Rare Earths* Vol. 20 (eds Gschneidner, K. A. & Eyring, L.) 207–291 (Elsevier, Amsterdam, 1995).
6. Mueller, W. M., Blackledge, J. P. & Libowitz, G. G. in *Metal Hydrides* (eds Mueller, W. M., Blackledge, J. P. & Libowitz, G. G.) Ch. 9 & 10 (Academic, New York, 1968).
7. Schlapbach, L. & Gupta, M. in *Hydrogen in Intermetallic Compounds* (ed. Schlapbach, L.) 139–217 (Topics in Appl. Phys. Vol. 63, Springer, Berlin, 1988).
8. Bonnet, J. E., Juckum, C. & Lucasson, A. *J. Phys. F: Met. Phys.* **12,** 699–711 (1982).
9. Pebler, A. & Wallace, W. A. *J. phys. Chem.* **66,** 148–151 (1962).
10. Lundin, C. E. & Blackledge, J. P. *J. Electrochem. Soc.* **109,** 838–842 (1962).
11. Flotow, H. E., Osborne, D. W. & Otto, K. *J. chem. Phys.* **36,** 866–872 (1962).
12. Yannopoulos, L. N., Edwards, R. K. & Wahlbeck, P. G. *J. phys. Chem.* **69,** 2510–2515 (1965).
13. Alefeld, G. *Ber. Bunsenges. phys. Chem.* **76,** 746–755 (1972).
14. Buccur, R. V. & Flanagan, T. B. *Z. phys. Chem.* **88,** 225–241 (1974).
15. Frazier, G. A. & Glosser, R. J. *J. Less-Common Met.* **74,** 89–96 (1980).
16. Lanford, W. A. *Nuc. Instrum. Meth.* **149,** 1–8 (1978).
17. Granqvist, C. G. in *Handbook of Inorganic Electrochromic Materials* (ed. Granquist, C. G.) Ch. 8, 9, 11 (Elsevier, Amsterdam, 1995).
18. Weaver, J. H., Rosei, R. & Peterson, D. T. *Phys. Rev.* B**19,** 4855–4866 (1979).
19. Peterman, D. J., Weaver, J. H. & Peterson, D. T. *Phys. Rev.* B**23,** 3903–3913 (1981).
20. Vajda, P. & Daou, J. N. *Phys. Rev. Lett.* **66,** 3176–3178 (1991).
21. Shinar, J., Dehner, B., Barnes, R. G. & Beaudry, B. J. *Phys. Rev. Lett.* **64,** 563–566 (1990).
22. Osterwalder, J. *Z. Phys.* B**61,** 113–128 (1985).
23. Bracconi, P., Pörschke, E. & Lässer, R. *Appl. Surf. Sci.* **32,** 392–408 (1988).
24. Switendick, A. C. *Int. J. Quant. Chem.* **5,** 459–470 (1971).
25. Dekker, J. P., van Ek, J., Lodder, A. & Huiberts, J. N. *J. Phys.: Cond. Mat.* **5,** 4805–4816 (1993).
26. Wang, Y. & Chou, M. Y. *Phys. Rev. Lett.* **71,** 1226–1229 (1993).
27. Zaanen, J., Sawatzky, G. A. & Allen, J. W. *Phys. Rev. Lett.* **55,** 418–421 (1985).
28. Halperin, B. I. & Rice, T. M. in *Solid State Physics* Vol. 21 (eds Seitz, F., Turnbull, D. & Ehrenreich, H.) 115–192 (Academic, New York, 1968).

ACKNOWLEDGEMENTS. We acknowledge discussions with G. Sawatzky, M. Kremens, P. H. L. Notten, P. A. Duine, H. van Houten, J. van de Ven, M. Ouwerkerk, F. J. A. den Broeder and P. J. Kelly. We thank B. Hjörvarsson, S. Olafsson and E. Karlsson for their help with the ^{15}N hydrogen profiling measurements. This work is part of the research programme of the Stichting voor Fundamenteel Onderzoek der Materie (FOM) which is supported by NWO.

Oxygen-isotope record of sea level and climate variations in the Sulu Sea over the past 150,000 years

Braddock K. Linsley*†

* Department of Geology and Geophysics, Rice University, Houston, Texas 77251, USA

THE Sulu Sea is located in the 'warm pool' of the western Pacific Ocean, where mean annual temperatures are the highest of anywhere on Earth. Because this large heat source supplies the atmosphere with a significant portion of its water vapour and latent heat, understanding the climate history of the region is important for reconstructing global palaeoclimate and for predicting future climate change. Changes in the oxygen isotope composition of planktonic foraminifera from Sulu Sea sediments have previously been shown to reflect changes in the planetary ice volume at glacial–interglacial and millenial timescales, and such records have been obtained for the late Pleistocene epoch and the last deglaciation[1–3]. Here I present results that extend the millenial time resolution record back to 150,000 years before present. On timescales of around 10,000 years, the Sulu Sea oxygen-isotope record matches changes in sea level deduced from coral terraces on the Huon peninsula[4]. This is particularly the case during isotope stage 3 (an interglacial period 23,000 to 58,000 years ago) where the Sulu Sea oxygen-isotope record deviates from the SPECMAP deep-ocean oxygen-isotope record[5]. Thus these results support the idea[4,6] that there were higher sea levels and less continental ice during stage 3 than the SPECMAP record implies and that sea level during this interglacial was just 40–50 metres below present levels. The subsequent rate of increase in continental ice volume during the return to full glacial conditions was correspondingly faster than previously thought.

The oxygen isotope ($\delta^{18}O$) data presented here are from Ocean Drilling Program (ODP) sites 769 and 768 in the Sulu Sea (Table 1, and Figs 1, 2 and 3). The $\delta^{18}O$ of the planktonic foraminifera *Globigerinoides ruber* was measured at ~400-yr resolution to develop a detailed palaeoclimate history of this region. Past work has shown that high-resolution sediment archives have been preserved at certain locations in the Sulu Sea owing to relatively high sediment accumulation rates[1–3] and reduced benthic mixing in the dysaerobic conditions of the deep basin[7].

The high quality and resolution of the Site 769 record is reflected in the preservation of both the full glacial–interglacial ice-volume amplitude and several millennial-scale climate events also found in higher-latitude palaeoclimate records. The glacial–interglacial $\delta^{18}O$ amplitude in this record (and other Sulu Sea records[3,8]) is only 1.3‰, almost equalling the 1.25‰ planetary ice-volume signal[9]. This indicates that the Sulu Sea experienced no significant change in sea surface temperatures (SSTs) between glacial and interglacial times, a conclusion also in agreement with recent foraminifera transfer function results from the western tropical Pacific which show that SST differed by less than 2 °C from the present[10].

The potentially most significant aspect of the Site 769 isotope record is its implications for eustatic sea level and planetary ice volume during interglacial isotope stage 3 (~23 to ~58 kyr ago). Throughout stage 3, relative $\delta^{18}O$ values at Site 769 are 0.5‰ more negative than the SPECMAP[5] composite deep-ocean $\delta^{18}O$ record which is thought to reflect global ice-volume changes (Fig. 3*a*). Instead, during stage 3, and throughout the 150-kyr record, Sulu Sea planktonic $\delta^{18}O$ is closely correlated with the sea-level record derived from Huon peninsula coral terraces[4] (Fig. 3*a*). This correlation, in conjunction with the 1.3‰ glacial–interglacial $\delta^{18}O$ amplitude, suggests that the lower-frequency components

† Present address: Department of Geological Sciences, University at Albany, State University of New York, Albany, New York 12222, USA.

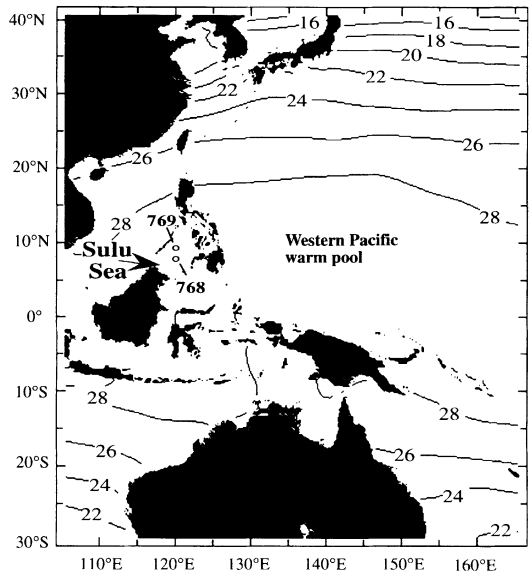

FIG. 1 Map showing the location of Ocean Drilling Program (ODP) sites 769 and 768 in the Sulu Sea. Annually averaged sea surface temperature (SST) contours (in °C)[32] are also shown, highlighting the area of the western Pacific warm pool. In the Sulu Sea, modern SSTs average ~28.5 °C and have an annual range from 26.5 to 30.5 °C. The basin is surrounded by a shallow sill which is mostly <100 m deep. Today, there is an open exchange of surface water between the Sulu Sea and surrounding seas[32,33] over the shelf and through channels (200–400 m deep) that connect the basin to the South China and Celebes seas. SST fields in the Sulu Sea indicate that the coldest waters occur in winter months (November–February), the result of through-flow across the Philippine archipelago from the open western Pacific[32,33]. Although Pleistocene sea level low stands would have exposed much of the sill surrounding the basin, previous studied have shown that the basin was never completely isolated[1,2]. Site 769 was cored above the basins carbonate lysocline[8] at 3,643 m on an isolated bathymetric high, and Site 768 was cored at 4,300 m in the Sulu Sea central deep basin.

of this $\delta^{18}O$ record are primarily a function of global ice-volume and sea-level variations.

The agreement between Site 769 $\delta^{18}O$ and the Huon terrace estimates of sea level during stage 3 (Fig. 3*a*) is particularly interesting, as these two records indicate significantly less global ice volume than does the deep-ocean $\delta^{18}O$ signal, even when this last signal is corrected for suspected cooler temperatures[6]. The relatively low $\delta^{18}O$ recorded by planktonic foraminifera in the Sulu Sea during stage 3 is apparently unique, and has not been reported in other western tropical Pacific locations such as the Banda Sea[11] or South China Sea[12]. However, both of these basins are more open to through-flow from the western Pacific. Perhaps the semi-isolated configuration of the basin has insulated the Sulu Sea from oceanographic changes, preserving the true ice-volume/sea-level signal. Alternatively, Sulu Sea surface waters during stage 3 could have become warmer and/or have had lower salinity with respect to the deep ocean and ice-volume signal. But the close correspondence between the sea-level curve derived from the Huon peninsula coral terraces[4] and Site 769 $\delta^{18}O$, coupled with the 1.3‰ glacial–interglacial $\delta^{18}O$ amplitude, argues against this and suggests that Site 769 $\delta^{18}O$ is a good proxy for sea-level changes with little effect of changes in local SST and/or $\delta^{18}O$ of sea water. Although the dating of some Huon corals may be affected by diagenetic alteration[13], the relative terrace elevations are accurate. In agreement with these results, further evidence for relatively high sea levels during stage 3 comes from submerged speleothems in the Bahamas[14].

In addition to the ice-volume/sea-level component, the Sulu Sea $\delta^{18}O$ values document several pronounced millennial-scale oceanographic events that reflect climate changes in the warm pool. Both cores 769 and 768 show 0.4‰ $\delta^{18}O$ decreases just before and after the Younger Dryas chronozone (YD), indicating the basin-wide coherence of the planktonic $\delta^{18}O$ signal (Table 1 and Fig. 3*b*). The radiocarbon-dated portions of both sites 769 and 768 show that the largest deglacial $\delta^{18}O$ shift correlates with the deep ocean and Northern Hemisphere records (Table 1 and Fig. 3), in contrast to the results from the Byrd Antarctic ice core which indicate that deglacial warming in Antarctica began ~3,000 yr before the onset of the warming in Greenland[15]. This suggests that the Sulu Sea was responding primarily to Northern Hemisphere climate changes at this time. Site 769 $\delta^{18}O$ also reveals other abrupt climate shifts that closely match those in Greenland and Antarctic ice cores (Fig. 3*b*)[16,17]. Most notably, similar events are observed at the isotope stage 5/4 glacial inception, and during interglacial stage 5e (Eemian). In addition, the $\delta^{18}O$ values from Site 769 show a pronounced 'step' at the stage 6/5 glacial transition, similar to that observed during the YD in this core.

A question posed by the presence of abrupt deglacial climate events in the Sulu Sea that are close in age to previously identified events in the North Atlantic[17–20] and high latitudes[20–22] is whether these abrupt $\delta^{18}O$ events reflect local changes in surface ocean conditions or, like the long-term trend, reflect global changes in the $\delta^{18}O$ of sea water. The overall $\delta^{18}O$ record presented here provides some clues. If the large-scale glacial–interglacial climate changes of the past 150 kyr did not produce significant SST changes in the Sulu Sea, it seems unlikely that lower-amplitude climate changes, such as the YD, could reflect lowered SST. Instead, it seems more likely that this Sulu Sea $\delta^{18}O$ record is a passive recorder of these climate signals. One potential mechanism that has been suggested previously, and which would explain these deglacial events, is advection along the sea surface (or through the atmosphere) of ^{18}O-depleted melt water from higher latitudes[23,24].

To explain the abrupt increases in planktonic $\delta^{18}O$ at the 5/4 boundary and during interglacial stage 5e, (a) different mechanism(s) must be invoked because ice sheets were greatly reduced in size or growing at these times. One possibility is that these two events may be related to oceanographic changes due to volcanism. I note that the large-scale Toba eruption in Sumatra occurred at ~75 kyr, at the stage 5/4 climate boundary[25]. This is also the same

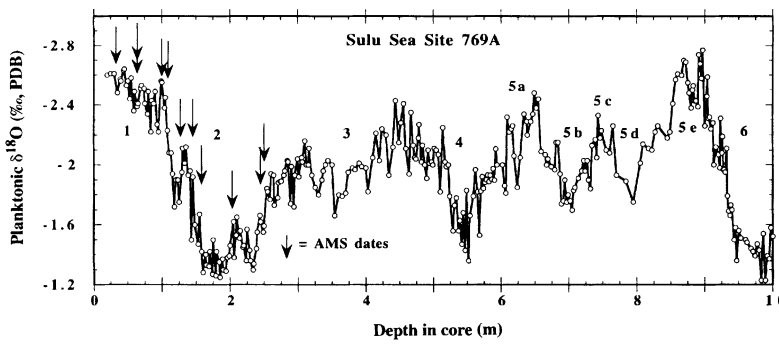

FIG. 2 Oxygen isotope analysis ($\delta^{18}O$ values) of the surface-dwelling planktonic foraminifera *Globigerinoides ruber* from ODP Site 769, plotted against depth in core. The upper 10 m of Site 769 was sampled at ~3-cm intervals for this study. Methods for the isotopic analyses are presented elsewhere[1,2]. Numbers indicate marine isotope stages. Vertical arrows mark the position of accelerator mass spectrometry (AMS) radiocarbon ages shown in Table 1. (Here $\delta^{18}O = [(^{18}O/^{16}O)_{sample}/(^{18}O/^{16}O)_{standard}] - 1$, where the PDB standard is used.)

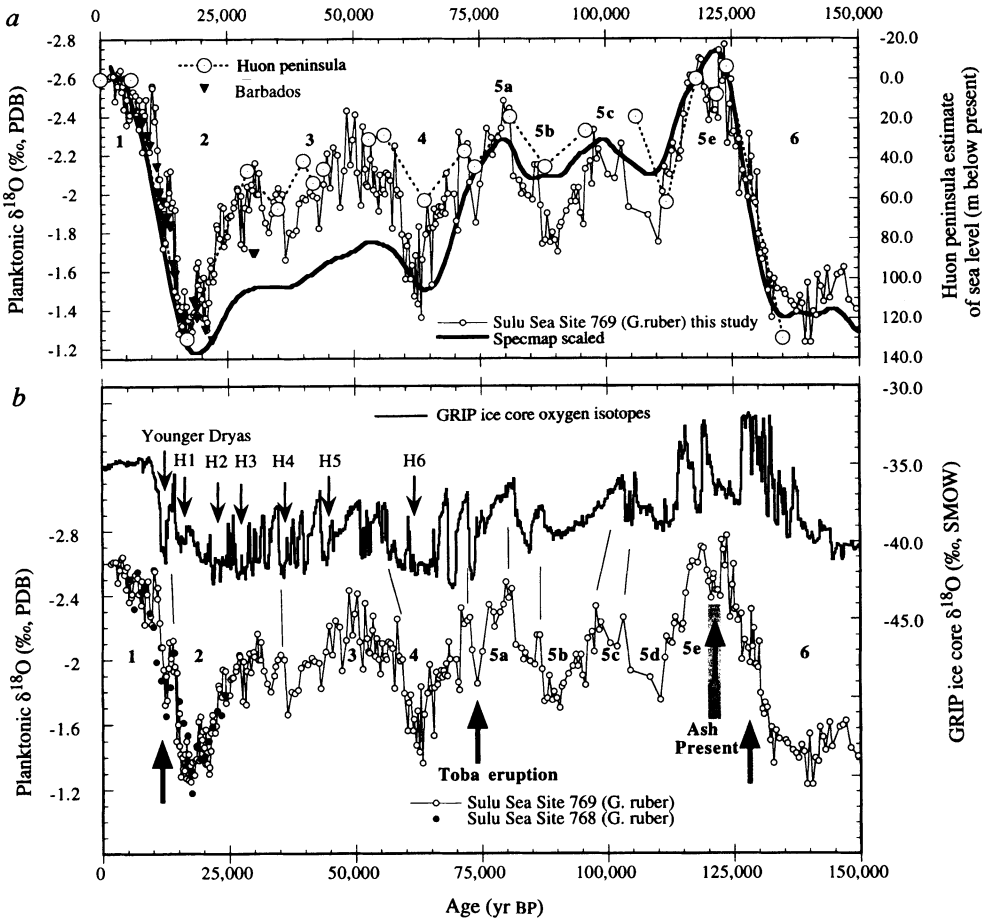

FIG. 3 *a*, ODP Site 769 planktonic $\delta^{18}O$ results (thin solid line with open circles) compared to a scaled version of the SPECMAP deep-ocean $\delta^{18}O$ record (bold solid line), and past sea level estimated from the Huon peninsula[4] (dashed line, large open circles) and Barbados[9,34] (filled triangles). Numbers indicate isotope stages. Note the close correspondence between the Huon peninsula sea-level record and Site 769 $\delta^{18}O$, in particular during stage 3 when the SPECMAP record is ~0.5‰ less negative. See text for discussion. *b*, Lower curve, oxygen isotope ($\delta^{18}O$) analyses from Sites 769 (thin line, open circles) and 768 (filled circles) plotted against time based on the age model given in Table 1. Large arrows mark locations of intervals discussed in the text, and numbers indicate the marine isotope stages. Upper curve, GRIP Greenland summit ice-core $\delta^{18}O$ results spanning the past 150,000 yr (ref. 17). The temporal position of the Younger Dryas and Heinrich events H1–H6 are marked by small arrows.

time as North Atlantic deep-water reorganization[26], a decrease in arboreal pollen in the Grande Pile peat record[27], and an increase in Vostok ice core δD (ref. 28). Evidence for stage 5e volcanism near the Sulu Sea comes from a minor amount of fine-grained sedimentary volcanic ash (63–250 μm) that is present during the brief interval of higher $\delta^{18}O$ values at ~122 kyr in Site 769 (Fig. 3*b*). This event suggests climate instability during the last interglacial in the western Pacific, as indicated by some (but not all) higher-latitude palaeoclimate records[17,27,29].

The lack of well defined events of lower $\delta^{18}O$ in the Sulu Sea during stage 3 may indicate that the volume of ^{18}O-depleted melt water associated with the stage 3 Dansgaard–Oeschger oscillations[19] was less than the volume of melt water released during deglacial events at the stage 2/1 and 6/5 boundaries. This interpretation also agrees with the evidence (from the Sulu Sea $\delta^{18}O$ values and the Huon peninsula sea-level record) of higher sea levels and less continental ice during stage 3 than implied by the SPECMAP deep-ocean $\delta^{18}O$ record. In turn, the Site 769 results independently corroborate the sea-level record derived from the Huon coral terraces[4] and support deep-ocean cooling and/or salinity effects on open-ocean benthic $\delta^{18}O$ records during stage 3 (ref. 6). These results also imply that continental ice build-up to full glacial conditions following stage 3 occurred at a higher rate, and within only a period

TABLE 1 Age models for sites 769 and 768

ODP site	Depth in core (cm)	AMC ^{14}C age (^{14}C yr BP)	Error*	Corrected age (cal. yr. BP)†	Species	SPECMAP age (cal. yr. BP)
769	0.31	3,180	60	2,613	*G. sacculifer*	–
769	0.62	5,430	65	5,178	*G. ruber*	–
769	0.62 dup.	5,515	70	5,275	*G. sacculifer*	–
769	1.01	9,550	95	10,422	*G. sacculifer*	–
769	1.07	10,120	80	11,151	*G. ruber*	–
769	1.28	11,500	185	12,901	*G. ruber*	–
769	1.45	12,950	135	14,716	*G. sacculifer*	–
769	1.6	13,450	110	15,336	*G. sacculifer*	–
769	2.05	16,400	135	18,935	*G. ruber*	–
769	2.45	18,720	155	21,694	*G. ruber*	–
769	2.5	19,275	150	22,345	*G. sacculifer*	–
769	5.2	–	–		–	59,000
769	6.1	–	–		–	71,000
769	6.5	–	–		–	80,000
769	7.5	–	–		–	99,000
769	7.9	–	–		–	110,000
769	8.5	–	–		–	115,000
769	9.1	–	–		–	126,000
768	0.85	9,740	80	10,665	*G. sacculifer*	–
768	1.05	12,525	80	14,187	*G. sacculifer*	–

* Error given is 1σ.

† Calendar year calculated following ref. 30 for raw uncorrected ages <9,000 ^{14}C yr, and following ref. 31 for raw ages >9,000 ^{14}C yr. Sedimentation rates for the radiocarbon-dated portion of the Site 769 record average 11.2 cm kyr^{-1}, whereas over the entire record sedimentation rates average 7.5 cm kyr^{-1}.

of ~10 kyr, much more rapidly than the deep-ocean $\delta^{18}O$ record indicates. □

Received 31 May 1995; accepted 14 February 1996.

1. Linsley, B. K. & Thunell, R. C. *Paleoceanography* **5,** 1025–1039 (1990).
2. Linsley, B. K. & Dunbar, R. B. *Paleoceanography* **9,** 317–340 (1994).
3. Kudrass, H. R., Erienkeuser, H., Vollbrecht, R. & Weiss, W. *Nature* **349,** 406–409 (1991).
4. Chappell, J. & Shackleton, N. J. *Nature* **324,** 137–140 (1986).
5. Imbrie, J. *et al.* in *Milankovitch and Climate* (eds Berger, A. *et al.*) 269–305 (Reidel, Norwell, MA, 1984).
6. Shackleton, N. *J. Quat. Sci. Rev.* **6,** 183–190 (1987).
7. Kuehl, S. A., Fuglseth, T. J. & Thunell, R. C. *Mar. Geol.* **111,** 15–35 (1993).
8. Linsley, B. K., Thunell, R. C., Morgan, C. & Williams, D. F. *Mar. Micropaleon.* **9,** 395–418 (1985).
9. Fairbanks, R. G. *Nature* **342,** 637–642 (1989).
10. Thunell, R. C., Anderson, D., Gellar, D. & Miao, Q. *Quat. Res.* **41,** 255–264 (1994).
11. Ahmad, S. M., Guichard, F., Hardjawidjaksana, K., Adisaputra, M. K. & Labeyrie, L. D. *Mar. Geol.* **22,** 385–397 (1995).
12. Luejiang, W. & Pinxian, W. *Paleoceanography* **5,** 77–90 (1990).
13. Gallap, C., Edwards, R. L. & Johnson, R. G. *Science* **263,** 796–800 (1994).
14. Richards, D. A., Smart, P. L. & Edwards, R. L. *Nature* **367,** 357–360 (1994).
15. Sowers, T. & Bender, M. *Science* **269,** 210–214 (1995).
16. Bender, M. *et al. Nature* **232,** 663–666 (1994).
17. Greenland Ice-Core Project (GRIP) Members *Nature* **364,** 203–207 (1993).
18. Bond, G. *et al. Nature* **365,** 143–147 (1993).
19. Dansgaard, W. *et al. Nature* **364,** 218–220 (1993).
20. Broecker, W. S. *Nature* **372,** 421–424 (1994).
21. Mathewes, R. W., Heusser, l. E. & Patterson, R. T. *Geology* **21,** 101–104 (1993).
22. Denton, G. H. & Hendy, C. H. *Science* **264,** 1434–1437 (1994).
23. Duplessy, J. C. *et al. Earth planet. Sci. Lett.* **103,** 27–40 (1991).
24. Anderson, D. M. & Thunell, R. C. *Quat. Sci. Rev.* **12,** 465–473 (1993).
25. Ninkovitch, D., Shackleton, N. J., Abek-Monem, A. A., Obradovitch, J. D. & Izett, G. *Nature* **276,** 574–577 (1978).
26. Keigwin, L. D. & Jones, G. A. *J. geophys. Res.* **99,** 12397–12410 (1994).
27. Thouveny, N. *et al. Nature* **371,** 503–506 (1994).
28. Jouzel, J. *et al. Nature* **329,** 403–408 (1987).
29. Field, M. H., Huntley, B. & Muller, H. *Nature* **371,** 779–783 (1994).
30. Stuiver, M. & Braziunas, T. F. *Radiocarbon* **35,** 137–189 (1993).
31. Bard, E., Arnold, M., Fairbanks, R. G. & Hamelin, B. *Radiocarbon* **35,** 191–199 (1993).
32. Levitus, S. & Boyer, T. P. *NOAA Atlas NESDIS 4* (US Dept of Commerce, US Govt Printing Office, Washington DC, 1994).
33. Wyrtki, K. *NAGA-Rep. No. 2* (Univ. California, La Jolla, 1961).
34. Bard, E., Hamelin, B. & Fairbanks, R. G. *Nature* **346,** 456–458 (1990).

ACKNOWLEDGEMENTS. I thank R. B. Dunbar for guidance and use of the stable-isotope facility at Rice University and R. C. Thunell for initiating earlier Sulu Sea research. This work was supported by the US National Science Foundation.

Constraints from partitioning experiments on the composition of subduction-zone fluids

Hans Keppler

Bayerisches Geoinstitut, Universität Bayreuth, 95440 Bayreuth, Germany

The generation of calc-alkaline magmas in subduction zones is thought to be the most important mechanism for the growth of continental crust since the Proterozoic eon. It is widely assumed that most of these magmas are products of fluid-triggered melting in the mantle wedge above the subducted slab[1,2]. Fluid transport from the subducted slab into the zone of melting has also been invoked in order to explain many of the trace element and radiogenic isotope characteristics of calk-alkaline magmas[3–7]. Here I report experimental data on the partitioning of trace elements between fluids, silicate melts and minerals, which suggest that the agent responsible for the transport of trace elements in subduction zones may be an alkali-chloride-rich aqueous fluid. The data show that chemical transport by such a fluid can generate the trace element and isotope enrichment pattern typical for calc-alkaline magmas, including the enrichment of large ionic lithophile elements, lead and uranium, and the characteristic depletion in niobium and tantalum.

Figure 1*a* shows the type of trace-element enrichment pattern characteristic of subduction-zone volcanics. While the elements below the dashed line are slightly depleted relative to the abundances in mid-ocean-ridge basalts (MORBs), others are strongly enriched. In Fig. 1*a*, the elements are ordered in such a way that the compatibility during normal, fluid-absent melting increases to the right. The fact that the relative enrichment of elements does not correlate with this sequence means that it cannot be explained by a simple melting event involving only fractionation of elements between a silicate melt and solid minerals. Rather, fluid transport may be responsible for the observed pattern.

The most important constituent of the subduction zone fluids is certainly water[1,2]. However, oceanic sediments and altered basalts in the subducted slab have been in contact with sea water and therefore contain abundant chloride. As chloride readily substitutes for OH groups in minerals such as amphibole, it can be transported to the depth of amphibole dehydration[1,2] where it will be released as a component of the hydrous fluid. Two lines of evidence support the presence of a chloride-rich hydrous fluid in subduction zones: the strongly elevated chlorine concentrations in calc-alkaline magmas (460–2,000 p.p.m.; ref. 6) and the presence of highly saline fluid inclusions in subduction zone metasediments from Dora Maira[8]. Most importantly, numerous experimental studies have shown that the presence of chloride strongly increases fluid/mineral and fluid/melt partition coefficients for many trace elements, owing to the formation of ion pairs and undissociated complexes in supercritical solutions[9,10]. Using the concept of 'hard' and 'soft' bases and acids[11], one can even predict which elements should be preferentially mobilized by a chloridic fluid. Chloride, as a moderately hard base, should preferentially react with moderately hard acids, such as Rb^+, Ba^{2+}, Sr^{2+}, Pb^{2+}. On the other hand, extremely hard acids, such as Nb^{5+} and Ta^{5+}, are not expected to react with chloride and will therefore not be transported by the fluid.

To test whether chemical transport by pure water or by a chloride-rich fluid can explain the trace element abundances in subduction-zone volcanics, experimental data on the partitioning of trace elements between such fluids and the minerals of the slab and the mantle wedge are necessary. Direct measurements of such partition coefficients are very difficult[9,12] or impossible. The extremely small diffusion coefficients of many trace elements in solid minerals often make it impossible to attain equilibrium within realistic run durations. Another problem in direct measurements of fluid/melt partition coefficients is caused by the recrystallization and sometimes incongruent dissolution of the solids during the experiment. Recrystallization will almost always lead to the formation of fluid inclusions in the mineral studied. If a trace element is highly incompatible in a mineral, even traces of submicroscopic fluid inclusions can lead to errors of several orders of magnitude in the measured partition coefficients. Incongruent dissolution can lead to the formation of tiny amounts of accessory phases that strongly concentrate certain trace elements and complicate the interpretation of the experiments. Therefore, in the present study, the fluid/mineral partition coefficients ($D^{\text{fluid/mineral}}$) have been determined indirectly by measuring the partitioning of trace elements between a fluid and a silicate melt. Because this measurement involves two liquid phases, attainment of equilibrium is not a problem. The fluid/mineral partition coefficients can then be estimated using published mineral/melt partition coefficients[13,14,20–22] according to the equation $D^{\text{fluid/mineral}} = D^{\text{fluid/melt}}/D^{\text{mineral/melt}}$. Strictly, this equation only holds if the melt composition studied is in equilibrium with the mineral of interest. The most important carrier of incompatible elements both in the subducted oceanic crust and in the mantle wedge is clinopyroxene. Therefore, the partitioning of trace elements between hydrous fluids and an andesitic melt was measured at 1,040–1,100 °C and 3–20 kbar, as under these conditions, this melt is very close to saturation with clinopyroxene[15]. Although the melt is not simultaneously saturated with olivine, orthopyroxene, garnet and amphibole, the data can also be used to at least approximately determine the $D^{\text{fluid/mineral}}$ for these phases.

All experiments were carried out in Pt or Pt–5% Rh capsules with an initial weight ratio of melt to fluid of 1:1. Either pure H_2O